

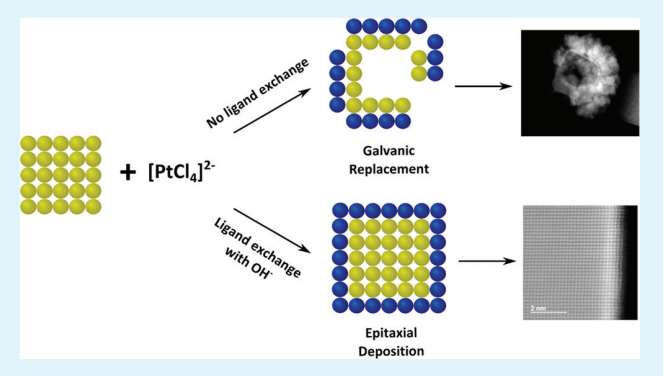
Addressing Challenges and Scalability in the Synthesis of Thin Uniform Metal Shells on Large Metal Nanoparticle Cores: Case Study of Ag-Pt Core-Shell Nanocubes

Umar Aslam[®] and Suljo Linic*

Department of Chemical Engineering, University of Michigan, Ann Arbor, Michigan 48109, United States

Supporting Information

ABSTRACT: Bimetallic nanoparticles in which a metal is coated with an ultrathin (~1 nm) layer of a second metal are often desired for their unique chemical and physical properties. Current synthesis methods for producing such core-shell nanostructures often require incremental addition of a shell metal precursor which is rapidly reduced onto metal cores. A major shortcoming of this approach is that it necessitates precise concentrations of chemical reagents, making it difficult to perform at large scales. To address this issue, we considered an approach whereby the reduction of the shell metal precursor was controlled through in situ chemical modification of the precursor. We used this approach to develop a highly scalable synthesis for coating atomic layers of Pt onto Ag



nanocubes. We show that Ag-Pt core-shell nanostructures are synthesized in high yields and that these structures effectively combine the optical properties of the plasmonic Ag nanocube core with the surface properties of the thin Pt shell. Additionally, we demonstrate the scalability of the synthesis by performing a 10 times scale-up.

KEYWORDS: core-shell, silver, platinum, scalable synthesis, ultrathin coating, ligand exchange

INTRODUCTION

The physical and chemical properties of bimetallic nanoparticles highly depend on the arrangement of atoms in the nanoparticles. 1-4 One commonly desired configuration is that of core-shell nanostructures in which a "core" metal is surrounded by a thin layer of a second metal. There are several appealing features to this architecture, including the following: (i) the shell metal can provide mechanical, thermal, or chemical stability for the core metal; (ii) the core of an expensive metal can be substituted for a cheap metal to reduce the overall cost; and (iii) the chemical reactivity of a shell metal can be perturbed by a core metal through a combination of ligand and strain effects. 5-9 Another emerging area of interest for metallic core/thin-shell nanoparticles involves combining the optical properties of a metal core with the surface properties of a shell metal. For example, nanoparticles of Cu, Ag, and Au are known to interact strongly with visible light through excitation of localized surface plasmon resonance (LSPR). 10-13 There is a great deal of interest in coating a plasmonic metal nanoparticle with a very thin layer of another metal as these core-shell nanostructures retain the optical properties of the plasmonic core while exhibiting surface properties associated with the shell metal. 14 These hybrid plasmonic structures could be useful for a number of applications such as surface-enhanced Raman spectroscopy, photothermal plasmonic heating, and plasmonic catalysis. 15,1

To take full advantage of the potential of these core/thinshell nanostructures, it is imperative to develop robust and scalable synthesis methods. Typically, the synthesis of bimetallic core-shell nanoparticles employs a seed-mediated approach whereby nanoparticles of the core metal are used as seeds and a metal precursor for the shell metal is deposited onto the seeds using a chemical reducing agent. ^{17–19} In general, this approach suffers from two potential drawbacks. The first issue is related to the scalability. To minimize side reactions such as uncontrolled homogeneous nucleation of the shell material, it is necessary to keep the concentration of the shell metal precursor in a mixture of seed cores very low. This is accomplished by very slow injection of the precursor into the mixture under strong reducing conditions. While this approach has been successfully implemented to coat thin layers of Au onto Ag, Pt onto Pd, and Ag-Pd onto Ag, it has also been recognized that it is difficult to implement such a synthesis at large scales as the reaction volume must be increased proportionally to maintain the appropriate low concentrations of all chemical reagents. 20-22 Another issue which affects some combinations of metals is related to the spontaneous galvanic

Received: September 24, 2017 Accepted: November 22, 2017

Published: November 22, 2017



ACS Applied Materials & Interfaces

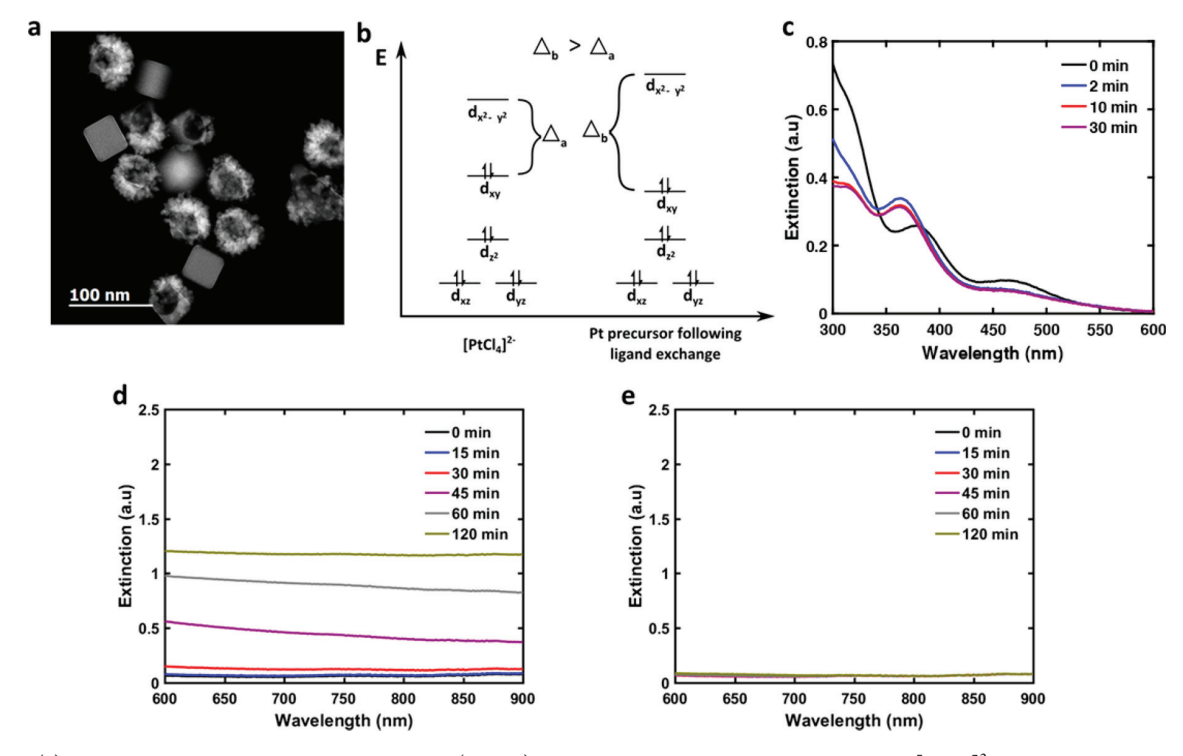


Figure 1. (a) Scanning transmission electron microscopy (STEM) image of Ag nanocubes after reacting with [PtCl₄]²⁻ precursor. Ag is oxidized by the Pt precursor, resulting in hollow nanostructures. (b) Energy diagram sketch of d-splitting for [PtCl₄]²⁻ metal complex and Pt precursor following ligand exchange with OH-. Hydroxide is a stronger field ligand than Cl-, resulting in a larger splitting between the orbitals. (c) UV-vis extinction of aqueous [PtCl₄]²⁻ following addition of NaOH solution. (d) Characterizing reduction of [PtCl₄]²⁻ by ascorbic acid. As the precursor is reduced to Pt metal, the solution turns black and optical extinction in the visible wavelength range increases. (e) Characterizing reduction of ligand-exchanged Pt^{2+} precursor. The visible optical extinction of the solution does not change over 2 h.

replacement of a core metal with the shell metal, which can lead to uncontrollable evolution of the nanostructure. 23,24

We recently reported, for the first time, a synthesis method for depositing a thin layer of Pt onto Ag nanocubes and demonstrated the usefulness of these nanostructures in plasmonic catalysis. 14 However, the procedure used in this prior work suffers from many of the above-mentioned constraints, making it tedious and difficult to perform the synthesis at large scales. Herein, we present a robust and easily scalable synthesis method for coating a thin layer of Pt onto Ag nanocube seeds. These bimetallic nanostructures are of interest as they combine the optical properties of Ag with the surface properties of Pt which makes them attractive for applications in plasmonic catalysis and surface-enhanced Raman spectroscopy. The synthesis of these Ag/Pt core/thin-shell nanostructures has proven to be very difficult since it requires controlling the homogeneous nucleation of Pt and the added challenge of preventing spontaneous galvanic replacement of Ag by Pt. 19,25 We show that by chemically modifying a Pt metal complex under the condition of synthesis, we can decrease the reduction potential of the Pt precursor, and in doing so prevent homogeneous reduction of the Pt metal precursor and the detrimental galvanic replacement of Ag by Pt. We demonstrate that this approach makes the synthesis much less sensitive to the concentration of chemical reagents in the reaction vessel, allowing large-scale syntheses to be performed. We also show that by employing this approach, we have excellent control of the Pt shell thickness ranging from 0.6 to 1.4 nm, and that we are able to synthesize high yields of the core-shell nanostructures with uniform Pt shell thickness.

RESULTS AND DISCUSSION

We first illustrate a shortcoming of a simple synthesis approach where preformed Ag nanocubes are used as seeds and a common Pt precursor (K₂PtCl₄) is reduced on the Ag nanocube seeds using a common mild reducing agent (ascorbic acid) at room temperature. If an aqueous solution of K₂PtCl₄ is added to an aqueous mixture of Ag nanocubes and ascorbic acid, atoms of Ag in the metal nanocubes will rapidly be oxidized through galvanic replacement with Pt resulting in the formation of hollow structures (Figure 1a). This detrimental side reaction is a consequence of the difference in the reduction potentials of the Pt metal complex $[PtCl_4]^{2-}$ and the reduction potential of the Ag oxidation product, $AgCl.^{26}$ Since the reduction potential of $[PtCl_4]^{2-}$ is higher than the reduction potential of AgCl, the replacement reaction of $2Ag + [PtCl_4]^{2-}$ \rightarrow 2AgCl + Pt + 2Cl⁻ is thermodynamically favorable. To avoid triggering this reaction, we explored using a Pt metal complex with a lower reduction potential than [PtCl₄]²⁻, thereby making the galvanic replacement reaction thermodynamically unfavorable.

To identify a Pt metal complex with the appropriate reduction potential, we considered a chemical modification of [PtCl₄]²⁻ through ligand exchange of the Cl⁻ ligands. [PtCl₄]²⁻ is a square planar d⁸ metal complex with a Pt²⁺ metal center requiring two electrons for reduction to Pt metal. In the framework of crystal field theory, the splitting of d-orbitals of the Pt²⁺ metal center can be changed by exchanging Cl⁻ ligands with other ligands, thereby changing the energy of the $5d_{x2-v2}$ orbitals (Figure 1b).²⁷ For example, if the Cl⁻ ligands are exchanged with stronger field-splitting ligands (such as OH⁻),

ACS Applied Materials & Interfaces

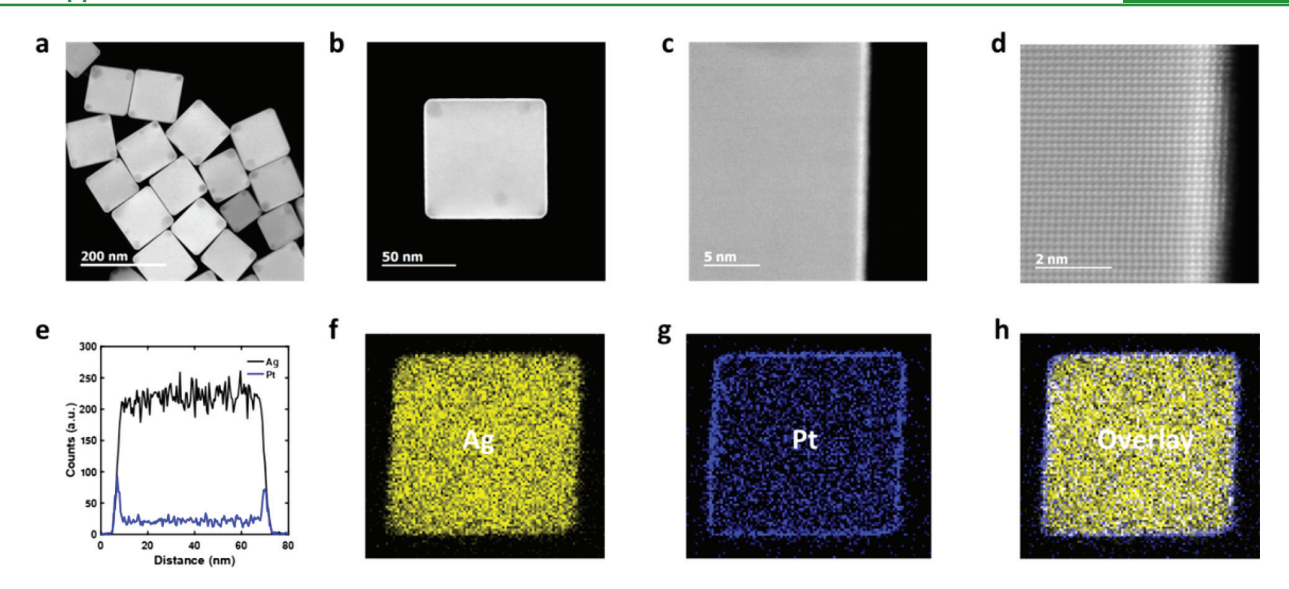


Figure 2. (a) STEM image of a collection of Ag-Pt core-shell nanocubes demonstrating high yield of core-shell structures, (b) a single Ag-Pt nanocube, (c) the edge of a single nanocube in which the \sim 1 nm Pt shell is clearly visible, and (d) atomic resolution image showing five atomic layers of Pt epitaxially deposited onto the Ag nanocube. (e) EDS elemental line scan across a representative Ag-Pt nanocube showing that the shell is made of Pt and the core of Ag. EDS elemental map of (f) Ag, (g) Pt, and (h) the overlay of the two.

then the energy level of the $Sd_{x^2-y^2}$ orbital will increase, thereby necessitating higher energy electrons to reduce Pt^{2+} to Pt metal (i.e., lowering the reduction potential of the complex), as depicted in Figure 1b.

To prepare a Pt metal precursor with lower reduction potential than $[PtCl_4]^{2-}$, we performed ligand exchange of a 4 mM aqueous solution of $[PtCl_4]^{2-}$ with OH^- by increasing the pH of the solution to $\sim\!12$ through addition of a NaOH solution. The high concentration of OH^- in solution promotes ligand exchange of the Cl^- ligands of $[PtCl_4]^{-2}$ with OH^- . UV—vis spectroscopy was used to characterize the ligand exchange. The data in Figure 1c show that the increase in the pH of the solution was accompanied by changes in the optical extinction by the metal complex, suggesting that the electronic structure of the metal complex changed through chemical interactions with OH^- ions. The changes to the metal precursor were complete after 10 min.

To test whether this ligand exchange affected the reducibility of the Pt2+ metal complex, an experiment was performed in which two aqueous solutions of 4 mM K₂PtCl₄ were reduced with 0.06 M ascorbic acid. The reactions were monitored using UV-vis spectroscopy. In the control sample, the pH of the solution was not adjusted and data in Figure 1d show that the reduction of the Pt precursor began taking place within 30 min of introducing the reducing agent. In the other sample, the solution pH was adjusted to ~12, and the solution containing the reducing agent (also kept at pH 12) was added after 10 min. As discussed above, these conditions allowed the precursor to undergo the above-described ligand exchange before the reducing agent was added. In contrast to the control sample, data in Figure 1e show there was no reduction of the Pt precursor for over 2 h after addition of the reducing solution. This suggests that the reduction potential of the Pt precursor is lowered following ligand exchange of Cl⁻ with OH⁻.

The chemically modified Pt precursor was then used for the synthesis of Ag-Pt core-shell nanocubes. Exact details of the synthesis protocol are provided in the Supporting Information document. The synthesis was performed by mixing 1 mL of a

solution containing Ag nanocube seeds (~0.7 mg/mL) with a solution of ascorbic acid and polyvinylpyrrolidone (PVP), a polymeric stabilizing agent. We note that we have also performed this synthesis with reducing agents other than ascorbic acid (see the Supporting Information document for associated discussion and data). The pH of the mixture was adjusted to ~12 with aqueous NaOH. The ligand-exchanged Pt²⁺ precursor was prepared as described above by increasing the pH of a 4 mM aqueous solution of K₂PtCl₄ to ~12 through addition of NaOH solution and allowing ligand exchange to occur for 10 min. The ligand-exchanged Pt²⁺ precursor solution was then added to the Ag nanocube mixture under stirring. This brought the final volume of the solution to 16 mL with a concentration of 2 mM ligand-exchanged Pt²⁺ precursor, 36 mM ascorbic acid, and 17 mM PVP at a pH of ~12. The mixture was allowed to react for 2 h. It was found that the pH of the solution gradually decreased over time possibly due to the consumption of ascorbate anions (i.e., the reducing agent) over time. As ascorbate anions are consumed, ascorbic acid dissociation will increase, thereby increasing the concentration of protons and lowering the pH. Because the chemical modification of the Pt^{2+} precursor is driven by a high concentration of OH^- (i.e., high pH), a decrease in pH causes the modified precursor to become unstable, resulting in the galvanic replacement of the Ag nanocubes by Pt. To avoid this, 25 μ L of a NaOH solution (1.25 M) was introduced to the reaction mixture every hour to maintain a high pH.

Scanning transmission electron microscopy (STEM) was used to characterize the Ag-Pt core—shell nanoparticles. Figure 2a shows a collection of Ag-Pt core—shell nanocubes, demonstrating that the nanostructures were produced in high yields with some etching at the corners of the nanocubes due to galvanic replacement of undercoordinated Ag atoms at the corners. A representative nanoparticle is shown in Figure 2b. An elemental line scan (Figure 2e) and elemental mapping (Figure 2f-h) performed using energy-dispersive X-ray spectroscopy (EDS) demonstrate that Pt atoms completely surround the cubic Ag core. The high resolution and atomic

resolution images in Figure 2c,d show that the average thickness of the Pt shell was 1.0 ± 0.1 nm, which corresponds to five atomic layers of epitaxially deposited Pt atoms. The thickness of the Pt shell could also be varied by changing the reaction time of the synthesis. For instance, a reaction time of 0.5 h produces a Pt shell thickness of 0.6 ± 0.1 nm and a reaction time of 8 h produces a 1.4 ± 0.1 nm thick shell of Pt (data shown in Figure S1). The slow, nonlinear increase in shell thickness with reaction time suggests that the initial reduction of Pt²⁺ onto the surface of the Ag nanocubes is relatively fast compared to the subsequent reduction of Pt²⁺ onto Pt surface atoms. This suggests that the surface Ag atoms are quickly coated with a layer of Pt which is followed by a much slower reduction of Pt²⁺ onto Pt surface atoms, resulting in the epitaxial growth of the Pt shell.

The optical properties of the core—shell nanoparticles were characterized using UV—vis extinction spectroscopy (Figure 3a). The optical extinction of the Ag nanocube seeds displays

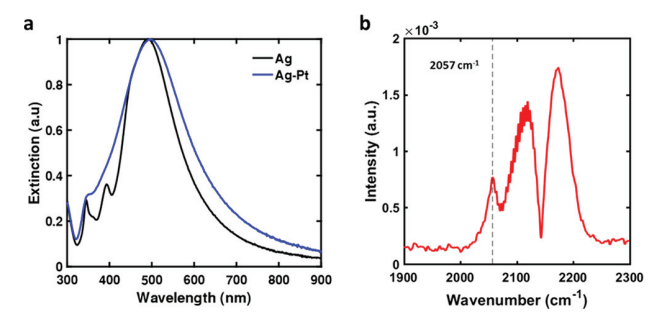


Figure 3. (a) Normalized optical extinction spectra of Ag nanocube seeds and Ag—Pt nanocubes. (b) DRIFTS data for CO adsorption on the surface of the Ag—Pt nanocubes. The feature centered at 2057 cm⁻¹ represents the vibrational frequency of the C—O bond when CO is adsorbed on the surface of the nanoparticles. The peaks at 2120 and 2170 cm⁻¹ are for residual gas-phase CO.

multiple peaks associated with dipolar, quadripolar, and higher order plasmon resonances. The data in Figure 3 show that when Pt is coated on the Ag nanocubes, the nanoparticles retain their plasmonic properties. The higher order plasmon resonance features are smeared and the main dipolar resonance peak is slightly broadened and red-shifted. The red shift in the plasmon peak can be attributed to a slight increase in the size of the nanoparticles as it is well-known that larger plasmonic nanoparticles have a lower energy LSPR frequency. The width of the peak is related to the decay rate of excited plasmons which increases when Pt is coated onto the Ag nanocubes due to an increase in absorption.

The chemical properties of the Ag–Pt nanocube surface were characterized by measuring the vibrational energy of CO adsorbed on the surface using diffuse reflectance infrared Fourier transform spectroscopy (DRIFTS). The nanoparticles were deposited onto a Si chip, treated with air at 250 °C for 3 h, and reduced with pure $\rm H_2$ at 200 °C for 1 h to clean the surface of the nanoparticles. A mixture of 10% CO in $\rm N_2$ was then flowed across the nanoparticles at room temperature for 10 min to allow CO to adsorb to the surface of the Ag–Pt nanocubes. Excess CO was then purged from the system using pure $\rm N_2$. Data in Figure 3b show a vibrational spectrum for adsorbed CO on Ag–Pt nanocubes. The vibrational frequency of the C–O bond when adsorbed on the surface of the Ag–Pt nanoparticles was measured to be at 2057 cm $^{-1}$ which is characteristic of CO

adsorbed on Pt surfaces. We note the vibrational energy of the C–O bond on spherical Pt nanoparticles (dominated by Pt(111) surface facet) is centered at 2060 cm^{-1,32} In contrast, the Ag–Pt nanocubes are dominated by the lower coordinated Pt(100) surface facet which causes the vibrational frequency of CO to be slightly lower.³³ The combination of the optical data and DRIFTS data in Figure 3 demonstrate that the Ag–Pt core–shell nanoparticles effectively combine the plasmonic properties of the Ag nanocube core with the surface properties of the Pt shell.

We have shown above that Ag-Pt core-shell nanocubes can be synthesized using a chemically modified Pt2+ precursor prepared through ligand exchange with OH-. The low reduction potential of the modified precursor prevents homogeneous nucleation of monometallic Pt nanoparticles and minimizes galvanic replacement of Ag by Pt. This characteristic makes the synthesis relatively insensitive to the concentration of Ag nanocube seeds or Pt2+ precursor, allowing for the synthesis to be easily performed at large scales without a substantial increase in the reactor volume. To demonstrate the scalability of the synthesis, a 10 times scale-up of the synthesis was performed following the procedure outlined above. After combining all reagents, the final volume of the reaction mixture was 20 mL which contained 10 mL of a solution of Ag nanocube seeds (~0.7 mg/mL), 4 mM of K₂PtCl₄, 70 mM ascorbic acid, and 90 mM of PVP at a pH of ~12. Despite the increase in concentration of the reducing agent, Pt2+ precursor, and 10 times increase in the number of Ag nanocube seeds, the epitaxial deposition of Pt onto the Ag nanocubes remained the most selective reaction pathway with no evidence of homogeneous nucleation of Pt nanoparticles and minimal galvanic replacement (Figure 4a). UV-vis spectroscopy was

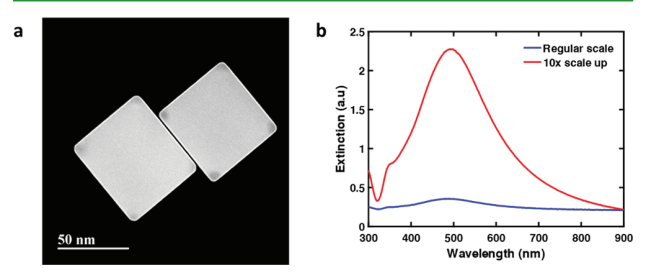


Figure 4. (a) STEM image of Ag—Pt nanocubes produced from 10 times scale-up synthesis. (b) UV—vis extinction spectra of Ag—Pt nanocubes in water demonstrating the success of the 10 times scale-up synthesis.

used to compare the concentration of the 10 times scale-up Ag–Pt product to the concentration of the small scale (\sim 0.7 mg of Ag nanocube seed) Ag–Pt product. Data in Figure 4 show that the maximum optical extinction for the scaled-up product was \sim 15 times higher than the maximum optical extinction for the regular scale product, clearly indicating that the scaled-up synthesis yielded at least a proportionally higher amount of the product Ag–Pt core—shell nanostructures.

CONCLUSION

We have developed a scalable synthesis approach for depositing a thin layer of Pt onto Ag nanocubes. This was accomplished using a synthesis in which the Pt²⁺ precursor was chemically modified through ligand exchange to decrease the precursor reduction potential. The low reduction potential of the

modified precursor minimized undesired side reactions such as homogeneous nucleation of Pt nanoparticles and galvanic replacement. This feature of the synthesis makes it relatively insensitive to the concentration of the chemical reagents, allowing for the synthesis to be easily scaled. As a demonstration of the scalability of the synthesis, we performed a 10 times scale-up without a substantial increase in the reaction vessel volume, using double the concentration of chemical reagents, and 10 times the amount of Ag nanocube seeds. The Ag-Pt nanocubes effectively couple the optical properties of Ag with the surface properties of Pt making them useful platforms for a number of applications including plasmonic catalysis, surface-enhanced Raman spectroscopy, photothermal heating, and others. The ability to easily synthesize these nanostructures at large scales should widen accessibility of these materials for such applications.

ASSOCIATED CONTENT

Supporting Information

The Supporting Information is available free of charge on the ACS Publications website at DOI: 10.1021/acsami.7b14474.

Exact synthesis details, characterization of varied shell thicknesses, use of other reducing agents, and use of other shell metal precursors (PDF)

AUTHOR INFORMATION

Corresponding Author

*E-mail: linic@umich.edu.

ORCID ®

Umar Aslam: 0000-0001-8310-2958

Notes

The authors declare no competing financial interest.

ACKNOWLEDGMENTS

Primary support for this work was provided by the U.S. Department of Energy, Office of Basic Energy Science, Division of Chemical Sciences (FG-02-05ER15686). Secondary support for developing analytical tools to study the optical properties of materials was provided by the National Science Foundation (NSF) (CBET-1702471 and CBET-1437601). The microscopy was supported by the University of Michigan College of Engineering and NSF (CBET-1436056, DMR-0723032, CHE-1362120). S.L. recognizes the partial support of the Institute for Advanced Study at Technische Universität München, funded by the German Excellence Initiative and the European Union Seventh Framework Programme under grant agreement no. 291763.

REFERENCES

- (1) Gilroy, K. D.; Ruditskiy, A.; Peng, H.-C.; Qin, D.; Xia, Y. Bimetallic Nanocrystals: Syntheses, Properties, and Applications. *Chem. Rev.* **2016**, *116* (18), 10414–10472.
- (2) Cortie, M. B.; McDonagh, A. M. Synthesis and Optical Properties of Hybrid and Alloy Plasmonic Nanoparticles. *Chem. Rev.* **2011**, *111* (6), 3713–3735.
- (3) Kitchin, J. R.; Nørskov, J. K.; Barteau, M. A.; Chen, J. G. Role of Strain and Ligand Effects in the Modification of the Electronic and Chemical Properties of Bimetallic Surfaces. *Phys. Rev. Lett.* **2004**, 93 (15), 156801.
- (4) Liz-Marzán, L. M.; Grzelczak, M. Growing Anisotropic Crystals at the Nanoscale. *Science* **2017**, *356* (6343), 1120–1121.
- (5) Niu, Z.; Cui, F.; Yu, Y.; Becknell, N.; Sun, Y.; Khanarian, G.; Kim, D.; Dou, L.; Dehestani, A.; Schierle-Arndt, K.; Yang, P. Ultrathin

- Epitaxial Cu@Au Core-Shell Nanowires for Stable Transparent Conductors. J. Am. Chem. Soc. 2017, 139 (21), 7348-7354.
- (6) Cleve, T. V.; Moniri, S.; Belok, G.; More, K. L.; Linic, S. Nanoscale Engineering of Efficient Oxygen Reduction Electrocatalysts by Tailoring the Local Chemical Environment of Pt Surface Sites. *ACS Catal.* **2017**, *7* (1), 17–24.
- (7) Xin, H.; Holewinski, A.; Linic, S. Predictive Structure—Reactivity Models for Rapid Screening of Pt-Based Multimetallic Electrocatalysts for the Oxygen Reduction Reaction. *ACS Catal.* **2012**, 2 (1), 12–16.
- (8) Schweitzer, N.; Xin, H.; Nikolla, E.; Miller, J. T.; Linic, S. Establishing Relationships Between the Geometric Structure and Chemical Reactivity of Alloy Catalysts Based on Their Measured Electronic Structure. *Top. Catal.* **2010**, *53* (5–6), 348–356.
- (9) Holewinski, A.; Idrobo, J.-C.; Linic, S. High-Performance Ag—Co Alloy Catalysts for Electrochemical Oxygen Reduction. *Nat. Chem.* **2014**, *6* (9), 828–834.
- (10) Linic, S.; Christopher, P.; Ingram, D. B. Plasmonic-Metal Nanostructures for Efficient Conversion of Solar to Chemical Energy. *Nat. Mater.* **2011**, *10* (12), 911–921.
- (11) Halas, N. J.; Lal, S.; Chang, W.-S.; Link, S.; Nordlander, P. Plasmons in Strongly Coupled Metallic Nanostructures. *Chem. Rev.* **2011**, *111* (6), 3913–3961.
- (12) Marimuthu, A.; Zhang, J.; Linic, S. Tuning Selectivity in Propylene Epoxidation by Plasmon Mediated Photo-Switching of Cu Oxidation State. *Science* **2013**, 339 (6127), 1590–1593.
- (13) Kelly, K. L.; Coronado, E.; Zhao, L. L.; Schatz, G. C. The Optical Properties of Metal Nanoparticles: The Influence of Size, Shape, and Dielectric Environment. *J. Phys. Chem. B* **2003**, *107* (3), 668–677.
- (14) Aslam, U.; Chavez, S.; Linic, S. Controlling Energy Flow in Multimetallic Nanostructures for Plasmonic Catalysis. *Nat. Nanotechnol.* **2017**, *12* (10), 1000–1005.
- (15) Huang, X.; El-Sayed, I. H.; Qian, W.; El-Sayed, M. A. Cancer Cell Imaging and Photothermal Therapy in the Near-Infrared Region by Using Gold Nanorods. *J. Am. Chem. Soc.* **2006**, *128* (6), 2115–2120
- (16) Linic, S.; Aslam, U.; Boerigter, C.; Morabito, M. Photochemical Transformations on Plasmonic Metal Nanoparticles. *Nat. Mater.* **2015**, *14* (6), 567–576.
- (17) Park, J.; Zhang, L.; Choi, S.-I.; Roling, L. T.; Lu, N.; Herron, J. A.; Xie, S.; Wang, J.; Kim, M. J.; Mavrikakis, M.; Xia, Y. Atomic Layer-by-Layer Deposition of Platinum on Palladium Octahedra for Enhanced Catalysts toward the Oxygen Reduction Reaction. ACS Nano 2015, 9 (3), 2635–2647.
- (18) Yang, Y.; Liu, J.; Fu, Z.-W.; Qin, D. Galvanic Replacement-Free Deposition of Au on Ag for Core—Shell Nanocubes with Enhanced Chemical Stability and SERS Activity. *J. Am. Chem. Soc.* **2014**, *136* (23), 8153—8156.
- (19) Sun, X.; Yang, Y.; Zhang, Z.; Qin, D. Mechanistic Roles of Hydroxide in Controlling the Deposition of Gold on Colloidal Silver Nanocrystals. *Chem. Mater.* **2017**, 29 (9), 4014–4021.
- (20) Xia, Y.; Gilroy, K. D.; Peng, H.-C.; Xia, X. Seed-Mediated Growth of Colloidal Metal Nanocrystals. *Angew. Chem., Int. Ed.* **2017**, 56 (1), 60–95.
- (21) Gao, C.; Lu, Z.; Liu, Y.; Zhang, Q.; Chi, M.; Cheng, Q.; Yin, Y. Highly Stable Silver Nanoplates for Surface Plasmon Resonance Biosensing. *Angew. Chem., Int. Ed.* **2012**, *51* (23), 5629–5633.
- (22) Li, J.; Liu, J.; Yang, Y.; Qin, D. Bifunctional Ag@Pd-Ag Nanocubes for Highly Sensitive Monitoring of Catalytic Reactions by Surface-Enhanced Raman Spectroscopy. *J. Am. Chem. Soc.* **2015**, *137* (22), 7039–7042.
- (23) Cobley, C. M.; Xia, Y. Engineering the Properties of Metal Nanostructures via Galvanic Replacement Reactions. *Mater. Sci. Eng., R* **2010**, 70 (3–6), 44–62.
- (24) Aslam, U.; Linic, S. Kinetic Trapping of Immiscible Metal Atoms into Bimetallic Nanoparticles through Plasmonic Visible Light-Mediated Reduction of a Bimetallic Oxide Precursor: Case Study of Ag–Pt Nanoparticle Synthesis. *Chem. Mater.* **2016**, 28 (22), 8289–8295.

- (25) Zhang, Y.; Liu, J.; Ahn, J.; Xiao, T.-H.; Li, Z.-Y.; Qin, D. Observing the Overgrowth of a Second Metal on Silver Cubic Seeds in Solution by Surface-Enhanced Raman Scattering. *ACS Nano* **2017**, *11* (5), 5080–5086.
- (26) Xia, X.; Wang, Y.; Ruditskiy, A.; Xia, Y. 25th Anniversary Article: Galvanic Replacement: A Simple and Versatile Route to Hollow Nanostructures with Tunable and Well-Controlled Properties. *Adv. Mater.* **2013**, 25 (44), 6313–6333.
- (27) Atkins, P. Shriver and Atkins' Inorganic Chemistry; OUP: Oxford, 2010.
- (28) Near, R.; Hayden, S.; El-Sayed, M. Extinction vs Absorption: Which Is the Indicator of Plasmonic Field Strength for Silver Nanocubes? *J. Phys. Chem. C* **2012**, *116* (43), 23019–23026.
- (29) Link, S.; El-Sayed, M. A. Size and Temperature Dependence of the Plasmon Absorption of Colloidal Gold Nanoparticles. *J. Phys. Chem. B* **1999**, 103 (21), 4212–4217.
- (30) Kreibig, U.; Vollmer, M. Optical Properties of Metal Clusters; Springer Science & Business Media: Berlin, 2013.
- (31) Maier, S. A. Plasmonics: Fundamentals and Applications; Springer Science & Business Media: Berlin, 2007.
- (32) Alayoglu, S.; Nilekar, A. U.; Mavrikakis, M.; Eichhorn, B. Ru–Pt Core–shell Nanoparticles for Preferential Oxidation of Carbon Monoxide in Hydrogen. *Nat. Mater.* **2008**, *7* (4), 333–338.
- (33) Kale, M. J.; Christopher, P. Utilizing Quantitative in Situ FTIR Spectroscopy To Identify Well-Coordinated Pt Atoms as the Active Site for CO Oxidation on Al2O3-Supported Pt Catalysts. *ACS Catal.* **2016**, *6* (8), 5599–5609.